

**Document Version**

Accepted author manuscript

**Citation (APA)**

Mirzaali Mazandarani, M., Van Dongen, I. C. P., Tümer, N., Weinans, H., Yavari, S. A., & Zadpoor, A. A. (2018). In-silico quest for bactericidal but non-cytotoxic nanopatterns. *Nanotechnology*, 29(43), Article 43LT02. <https://doi.org/10.1088/1361-6528/aad9bf>

**Important note**

To cite this publication, please use the final published version (if applicable). Please check the document version above.

**Copyright**

In case the licence states “Dutch Copyright Act (Article 25fa)”, this publication was made available Green Open Access via the TU Delft Institutional Repository pursuant to Dutch Copyright Act (Article 25fa, the Taverne amendment). This provision does not affect copyright ownership. Unless copyright is transferred by contract or statute, it remains with the copyright holder.

**Sharing and reuse**

Other than for strictly personal use, it is not permitted to download, forward or distribute the text or part of it, without the consent of the author(s) and/or copyright holder(s), unless the work is under an open content license such as Creative Commons.

**Takedown policy**

Please contact us and provide details if you believe this document breaches copyrights. We will remove access to the work immediately and investigate your claim.

1 Communication

2

3 *In-silico* quest for bactericidal but non-cytotoxic  
4 nanopatterns

5

6 M. J. Mirzaali<sup>a</sup>, I.C.P. van Dongen<sup>a,b</sup>, N. Tümer<sup>a</sup>, H. Weinans<sup>a,b,c</sup>,  
7 S. Amin Yavari<sup>b,\*</sup>, A. A. Zadpoor<sup>a,1</sup>

8

9 <sup>a</sup> *Department of Biomechanical Engineering, Faculty of Mechanical, Maritime, and Materials*  
10 *Engineering, Delft University of Technology (TU Delft), Mekelweg 2, 2628 CD, Delft, The*  
11 *Netherlands*

12 <sup>b</sup> *Department of Orthopedics, University Medical Centre Utrecht, Utrecht, The Netherlands*

13 <sup>c</sup> *Department of Rheumatology, University Medical Centre Utrecht, Utrecht, The Netherlands*

14

15

16

---

<sup>1</sup> Both authors share last authorship

\* Corresponding author

E-mail address: [s.aminyavari@umcutrecht.nl](mailto:s.aminyavari@umcutrecht.nl), [saber.aminyavari@gmail.com](mailto:saber.aminyavari@gmail.com)

1 **Abstract**

2 Nanopillar arrays that are bactericidal but not cytotoxic against the host cells could be used  
3 in implantable medical devices to prevent implant-associated infections. It is, however,  
4 unclear what heights, widths, interspacing, and shape should be used for the nanopillars to  
5 achieve the desired antibacterial effects while not hampering the integration of the device in  
6 the body. Here, we present an *in-silico* approach based on finite element modeling of the  
7 interactions between *Staphylococcus aureus* and nanopatterns on the one hand and  
8 osteoblasts and nanopatterns on the other hand to find the best design parameters. We found  
9 that while the height of the nanopillars seems to have little impact on the bactericidal  
10 behavior, shorter widths and larger interspacings substantially increase the bactericidal  
11 effects. The same combination of parameters could, however, also cause cytotoxicity. Our  
12 results suggest that a specific combination of height (120 nm), width (50 nm), and  
13 interspacing (300 nm) offers the bactericidal effects without cytotoxicity.

14 **Keywords:** Nanopattern design, implant-associated infections, osseointegration, finite  
15 element modelling.

16

1 Nanopillar arrays found on the wings of cicada and dragonfly behave as natural bactericidal  
2 surfaces [1]. The nanopillars penetrate into the bacterial walls or stretch them, resulting in  
3 cytoplasm leakage and cell death [2]. The nanopillars found on the wing of cicada have a  
4 height of 200 nm, a nanopillar interspacing of 170 nm, a width at the base of 100 nm, and a  
5 width at the cap of 60 nm [3]. Similar nanopatterned structures could be found on the wings  
6 of dragonfly with heights of 189-311 nm and widths of 37-57 nm [2]. Surfaces decorated  
7 with similar types of nanopatterns have been fabricated by researchers and are demonstrated  
8 to exhibit bactericidal behavior [4], [5].

9 Implantable medical devices could potentially be covered with such types of nanopatterns to  
10 protect patients against implant-associated infections (IAIs). In the case of orthopaedic  
11 implants, IAIs are one of the major factors limiting the longevity of implants [6], [7]. For  
12 example, 0.5-5% of the patients undergoing joint replacement surgeries experience IAIs [8].  
13 Many researchers are therefore developing coatings [9], surface treatments [10], [11], and  
14 hydrogels [12] to prevent the infections associated with orthopaedic surgeries. However,  
15 many of these coatings may elicit undesired effects such as cytotoxicity [13]. In comparison,  
16 nanopatterned surfaces offer a safer non-pharmaceutical alternative that could be harnessed  
17 to prevent IAIs.

18 A major research question when designing antibacterial nanopatterns is: ‘what are the best  
19 values for the height, diameter, and inter-spacing of the nanopillars such that the nanopatterns  
20 are bactericidal but not cytotoxic against host cells?’ Answering this question requires a  
21 systematic study of how different parameters influence both types of behaviors. The major  
22 challenge when performing such studies is accurate and reproducible fabrication of  
23 nanopatterns with different sets of design parameters. Nanoimprint lithography [14],

1 nanowires based on hydrothermal treatment [15], or deep reactive ion etching [16] have been  
2 currently in use for fabrication of nanopatterns. Most of these techniques are, however,  
3 costly, slow, and labor-intensive and need much calibration before they could be applied to  
4 new (metallic) materials. Here, we present an *in-silico* approach based on computational  
5 modeling of the cell-surface interactions to find the design parameters of nanopatterns.

6 We used a model of Gram-positive *Staphylococcus aureus* (*S. aureus*), which is a common  
7 bacterium in the human body and a major cause of bone and joint infections [17], to study  
8 the response of bacteria to nanopatterns. Osteoblasts are responsible for *de novo* bone  
9 formation and osseointegration of the implants [11]. Therefore, these cells were used for the  
10 simulations to study their response to nanopatterns with the goal to preserve them, i.e. no  
11 cytotoxicity behavior.

12 *S. aureus* is spherical in shape with a relatively thick wall consisting of peptidoglycans,  
13 which give the bacteria its shape and strength [18] (Figure 1a). The geometrical dimensions  
14 of the bacterial cell, i.e. the outer diameter ( $D = 600$  nm) and thickness ( $th = 10$  nm), were  
15 set according to the information available in the literature [19], [20]. Osteoblasts were  
16 modelled using polygons with a hat-shape for the cytoplasm and an ellipse shape for the  
17 nucleus (Figure 1a). The maximum diameter of the cytoplasm ( $D = 20$   $\mu$ m) and its thickness  
18 ( $th = 6$  nm) as well as the dimensions of the nucleus (Figure 1a) were chosen based on the  
19 values reported in the literature [21], [22].

20 A visco-hyperelastic material model (Neo-Hookean, viscoelastic) was used for modeling the  
21 cytoplasm of *S. aureus* [23], [24], while the cell wall was assumed to behave linear elastically  
22 [25], [26]. A linear elastic material model was used for modeling the nucleus and membrane  
23 of the osteoblast cells [22] and a similar visco-hyperelastic material model similar to the one

1 used for *S. aureus* was used for the modeling the cytoplasm of osteoblasts [21], [22], [24].  
2 *An analysis of the time period for the viscoelastic material properties was discussed in the*  
3 *supplementary document and Figure S1.* A summary of all parameters and their sources are  
4 presented in Table S1. A linear elastic material model ( $E = 150$  GPa,  $\nu = 0.278$  [27]) was  
5 used to describe the mechanical behavior of nanopillars. This was based on the assumption  
6 that nanopillar were made using electron beam induced deposition with platinum pre-cursors  
7 [28]. *We also considered different material properties for the nanopillars (see the*  
8 *supplementary document, Figure S2).*

9 We used a nonlinear implicit solver (Abaqus Standard 6.14) to simulate the models. 2D plane  
10 strain quadratic quadrilateral elements with hybrid deformation (CPE8H) and without  
11 (CPE8) were respectively used for meshing the cells and nanopillars. A mesh convergence  
12 analysis was performed (see the supplementary document, *Figure S3, and S4*) according to  
13 which a minimum element size of 3 nm and 10 nm were respectively used for modeling the  
14 *S. aureus* and osteoblast cells. An out-of-plane thickness of 600 nm and 20  $\mu\text{m}$  were  
15 considered in the modeling of *S. aureus* and osteoblast cell, respectively.

16 The finite element models simulated the conditions used in an *in vitro* experimental study of  
17 how bacteria interact with nanopatterned surfaces [29]. We assumed that cells experience  
18 two types of forces including their own weight and the forces caused by the height of the  
19 water (culture medium) column. The sum of both forces was applied as a body force. The  
20 buoyant forces were small in comparison and were, thus, neglected.

21 A variation of the height,  $H$ , width,  $W$ , interspace,  $IS$ , radius,  $r$ , and shape of the  
22 nanopatterned surfaces (Figure 1b) were used in the finite element models. To evaluate the  
23 effects of each design parameter on the deformation of cell walls/ membrane, the most

1 extreme values of each parameter found in the literature were implemented in the finite  
2 element models. For example, the smallest and largest values considered for the width,  $W$ ,  
3 were respectively 25 nm and 200 nm [11], [14], [16], [30].

4 A total mass of 1 pg was used for *S. aureus* [31]. A parametric study showed that the obtained  
5 overall stress/strain distributions are in general similar regardless of how the mass is  
6 distributed between the cell wall and cytoplasm (see the supplementary document for the  
7 details, [Figure S5](#)). We therefore assumed that the cytoplasm and cell walls equally  
8 contribute to the mass of the bacteria, applying 50% of the total body force to each  
9 compartment. The mass of the osteoblast cell is reported to be around 1.48 ng with different  
10 densities for its constituents, i.e.,  $\rho_{\text{nucleus}} = 1.8 \times 10^{-9}$  [ton/mm<sup>3</sup>],  $\rho_{\text{cytoplasm}} = 1.5 \times 10^{-9}$   
11 [ton/mm<sup>3</sup>], and  $\rho_{\text{membrane}} = 0.6 \times 10^{-9}$  [ton/mm<sup>3</sup>] [21], [22]. The body forces applied to the  
12 different parts of the cell models were determined accordingly (Table S2).

13 A nonlinear surface-to-surface contact type was considered for all the simulations with a  
14 rough frictional formulation for the tangential behavior and hard contact pressure-  
15 overclosure for the normal behavior. The contact type used enabled a smooth sliding of the  
16 cells into the area between the nanopillars. The different compartments of the cells were tied  
17 to each other. A strain-based failure criterion was used to predict a rupture in the cell wall  
18 (or membrane) of bacteria (or host cells). The bacteria and host cells were assumed to be  
19 killed if numerically calculated equivalent von Mises strain,  $\varepsilon_{eq}$ , in the cell wall or membrane  
20 exceeded threshold of  $\varepsilon_{th} = 0.5$  for *S. aureus* [32] and  $\varepsilon_{th} = 1.05$  for osteoblast [33].  
21 Furthermore, sinking depth ratio,  $SD/D$ , was defined as the maximum of deformation in the  
22 cell wall or membrane,  $SD$ , normalized to the diameter of the bacteria or cell,  $D$ .

1 The height of nanopillars did not substantially change the maximum equivalent strain  
2 experienced by the cell wall of the bacteria, meaning that height does not influence the  
3 bactericidal behavior of the nanopatterns (Figure 2a). However, a combination of the width  
4 and interspacing of the nanopillars caused high levels of variation in the maximum equivalent  
5 strain induced in the cell wall (Figure 2b, c). The von Mises strain and normalized sinking  
6 depth reached their maximum values when the minimum width was combined with the  
7 maximum value of the interspacing, i.e.,  $IS = 300$  nm and  $W = 200$  nm (Figure 2b, c). The  
8 effects of nanopillar shape on the equivalent von Mises strain were relatively limited (Figure  
9 2d). Smaller values of the relative radius,  $r/W$ , caused higher levels of von Mises strain  
10 (Figure 2e). *Change in the maximum stress of bacteria and the average stress in nanopillars*  
11 *are shown in Figure S6 of the supplementary document.*

12 The nanopillar designs that caused high equivalent von Mises strains in the bacteria cell wall  
13 were chosen to simulate their interactions with osteoblasts. We found that combining the  
14 largest values of nanopillar interspacing with the smallest widths could also result in  
15 cytotoxicity (Figure 3a-c). *Change of stress in the osteoblast cell and the nanopillars are*  
16 *depicted in Figure S7 of the supplementary document.* Increasing the width of the  
17 nanopillars, however, resulted only in bactericidal behavior but no cytotoxicity (Figure 3b  
18 and c). Two non-dimensional parameters  $\frac{W}{W+IS}$ , and  $\frac{R}{IS}$  showed strong correlation with the  
19 von Mises strain (Figure 3d, e) and may have some value as surrogate parameters when  
20 designing bactericidal nanopatterns. Taken together, the results of the current study point  
21 towards one specific combination of height, width, and interspacing to ensure the  
22 nanopatterns are bactericidal but not cytotoxic, i.e.  $W = 50$  nm, and  $IS = 300$  nm.

1 The diameters of the nanopillars for which bactericidal effects are predicted are between 25  
2 nm and 50 nm. These values are within the range of the diameter of nanopatterns that have  
3 been shown to be bactericidal against *S. aureus* [34]. These numerically estimated diameters  
4 are also comparable with those found for the dragon fly wing (50-70 nm) that are known to  
5 be bactericidal against *S. aureus* [34]. Au nanostructured surface with diameters of 50 nm  
6 [30] has also been found to kill *S. aureus*, which is in line with our simulation results. In  
7 terms of nanopillar interspacing, the values reported in the literature for bactericidal  
8 nanopatterns are usually higher than 100 nm and in the range of 150-300 nm [35]. Not much  
9 experimental data regarding the cytotoxicity of the above-mentioned nanopatterns is  
10 available in the literature. In one study, nanopillar arrays with an interspacing of 300 nm and  
11 a small width at the top (triangular shape pillars) reduced the attachment of mammalian cells  
12 [36]. These experimental values are comparable to those for which our models predict  
13 cytotoxic behavior (i.e. a diameter of 25 nm and an interspacing of 300 nm).

14 Systematic study of both bactericidal and cytotoxic behaviors is one of the unique properties  
15 of the current study. The next step will consist of experiments in which these predicted design  
16 values will be used for evaluating their behavior against bacteria and host cells. Although the  
17 predictions of our computational models are in line with experimental findings, the more  
18 general trends may be only valid within the ranges for which we have actually run the  
19 simulations. For example, a nanopillar tip much sharper than those considered here may kill  
20 bacteria. Very sharp nanopillars create singularity in elastic simulations and were therefore  
21 avoided. Moreover, sharpest nanopillars are almost certain to be also cytotoxic, as the  
22 singular strains experienced at the top most probably will exceed the limit allowable for  
23 mammalian cells as well. The trend observed here regarding the height of the nanopillars is

1 only valid when the sinking depth of the bacteria is smaller than the height of the nanopillars  
2 in which case the cell does not feel the extra height of the nanopillars. If the sinking depth  
3 goes beyond the height of the nanopillars, larger heights are expected to increase the  
4 deformation and, thus, the bactericidal behavior.

5 *We changed the mechanical properties of the nanopillars within three orders of magnitude*  
6 *(i.e. 150 GPa to 150 MPa). This spans the properties of a wide range of relevant materials*  
7 *including titanium and hydroxyapatite. These further simulations have been performed for*  
8 *the cases that showed a bactericidal effect, i.e.,  $W = 25$  and  $W = 50$  with  $IS = 300$ . The*  
9 *conclusions regarding the bactericidal behavior and cytocompatibility of the nanopatterns*  
10 *remained unchanged regardless of the elastic modulus used.*

11 *It is worth mentioning that in this study we only focused on the simulation of Gram-positive*  
12 *bacteria (*S.aureus*) and not Gram-negative ones. *S.aureus* is a major cause of infections*  
13 *associated with orthopaedic implants. The Gram-positive and Gram-negative bacteria have*  
14 *different membrane compositions. The Gram-positive bacteria have a thicker cell wall*  
15 *(between 20-80 nm) composed of peptidoglycan and teichoic, which makes for a more rigid*  
16 *cell wall as compared to the Gram-negative bacteria that have a thinner outer membrane*  
17 *(8-12 nm) made up of peptidoglycan [38], [39]. Due to these differences, Gram-negative*  
18 *bacteria are chemically tougher than the Gram-positive ones but mechanically Gram-*  
19 *negative bacteria are weaker. Since our computational models do not take the chemical*  
20 *interaction of these cells with nanopatterns into account, we believe that the results presented*  
21 *for the Gram-positive bacteria in this study provides an upper bound for both cell types.*

22

1 In this study, we only considered the gravitational force and the pressure caused by the water  
2 column. The adhesion forces between the bacterium and nanopillars [2], [26], [37], [38] and  
3 the resulting shear forces were not taken into account. Hydrophilic surface properties have  
4 been also proposed as another mechanism affecting the bactericidal properties of  
5 nanopatterns [3], [35], which were not studied here. *From our simulations, it is not clear how  
6 much these shear forces and mechanisms individually contribute to the fate of cells.  
7 However, to have a realistic simulation of cytotoxic/ bactericidal activity, all of these  
8 mechanisms should be taken into account. Furthermore, in this study, we only focused on the  
9 contact killing mechanism, while neglecting other chemical mechanisms for killing the  
10 bacteria.*

11 In summary, we developed an *in-silico* approach for finding the best design parameters of  
12 nanopillar arrays such that the nanopatterns exhibit bactericidal behavior but are not  
13 cytotoxic against host cells. Our finite element models predict that the width and interspacing  
14 of the nanopillars are the most important parameters influencing the bactericidal behavior of  
15 such arrays. We also found a specific combination of width and interspacing, i.e.  $W =$   
16  $50\text{ nm}$ , and  $IS = 300\text{ nm}$ , that our models predict to be bactericidal but not cytotoxic for  
17 host osteoblasts. The proposed nanopatterns can now be tested e.g. on the titanium surface  
18 of joint implants to prevent implant infection and not harm bony ingrowth.

## 19 **Competing Interests**

20 The authors declare that they have no competing interests.

## 21 **REFERENCES**

- 22 [1] E. P. Ivanova, J. Hasan, H. K. Webb, V. K. Truong, G. S. Watson, J. A. Watson, V.  
23 A. Baulin, S. Pogodin, J. Y. Wang, M. J. Tobin, and others, "Natural bactericidal  
24 surfaces: mechanical rupture of *Pseudomonas aeruginosa* cells by cicada wings,"  
25 *Small*, vol. 8, no. 16, pp. 2489–2494, 2012.

- 1 [2] C. D. Bandara, S. Singh, I. O. Afara, A. Wolff, T. Tesfamichael, K. Ostrikov, and A.  
2 Oloyede, “Bactericidal effects of natural nanotopography of dragonfly wing on  
3 *Escherichia coli*,” *ACS applied materials & interfaces*, vol. 9, no. 8, pp. 6746–6760,  
4 2017.
- 5 [3] A. Elbourne, R. J. Crawford, and E. P. Ivanova, “Nano-structured antimicrobial  
6 surfaces: From nature to synthetic analogues,” *Journal of colloid and interface  
7 science*, vol. 508, pp. 603–616, 2017.
- 8 [4] J. A. Inzana, E. M. Schwarz, S. L. Kates, and H. A. Awad, “Biomaterials approaches  
9 to treating implant-associated osteomyelitis,” *Biomaterials*, vol. 81, pp. 58–71, 2016.
- 10 [5] R. Kuehl, P. S. Brunetto, A.-K. Woischnig, M. Varisco, Z. Rajacic, J. Vosbeck, L.  
11 Terracciano, K. M. Fromm, and N. Khanna, “Preventing implant-associated  
12 infections by silver coating,” *Antimicrobial agents and chemotherapy*, vol. 60, no. 4,  
13 pp. 2467–2475, 2016.
- 14 [6] A. de Breij, M. Riool, P. H. Kwakman, L. de Boer, R. A. Cordfunke, J. W. Drijfhout,  
15 O. Cohen, N. Emanuel, S. A. Zaat, P. H. Nibbering, and others, “Prevention of  
16 *Staphylococcus aureus* biomaterial-associated infections using a polymer-lipid  
17 coating containing the antimicrobial peptide OP-145,” *Journal of Controlled Release*,  
18 vol. 222, pp. 1–8, 2016.
- 19 [7] J. Raphel, M. Holodniy, S. B. Goodman, and S. C. Heilshorn, “Multifunctional  
20 coatings to simultaneously promote osseointegration and prevent infection of  
21 orthopaedic implants,” *Biomaterials*, vol. 84, pp. 301–314, 2016.
- 22 [8] D. Campoccia, L. Montanaro, and C. R. Arciola, “The significance of infection  
23 related to orthopedic devices and issues of antibiotic resistance,” *Biomaterials*, vol.  
24 27, no. 11, pp. 2331–2339, 2006.
- 25 [9] I. A. van Hengel, M. Riool, L. E. Fratila-Apachitei, J. Witte-Bouma, E. Farrell, A. A.  
26 Zadpoor, S. A. Zaat, and I. Apachitei, “Selective laser melting porous metallic  
27 implants with immobilized silver nanoparticles kill and prevent biofilm formation by  
28 methicillin-resistant *Staphylococcus aureus*,” *Biomaterials*, vol. 140, pp. 1–15, 2017.
- 29 [10] S. Amin Yavari, L. Loozen, F. L. Paganelli, S. Bakhshandeh, K. Lietaert, J. A. Groot,  
30 A. C. Fluit, C. Boel, J. Alblas, H. C. Vogely, and others, “Antibacterial behavior of  
31 additively manufactured porous titanium with nanotubular surfaces releasing silver  
32 ions,” *ACS applied materials & interfaces*, vol. 8, no. 27, pp. 17080–17089, 2016.
- 33 [11] S. Dobbenga, L. E. Fratila-Apachitei, and A. A. Zadpoor, “Nanopattern-induced  
34 osteogenic differentiation of stem cells—A systematic review,” *Acta biomaterialia*,  
35 vol. 46, pp. 3–14, 2016.
- 36 [12] S. Bakhshandeh, Z. Gorgin Karaji, K. Lietaert, A. C. Fluit, C. E. Boel, H. C. Vogely,  
37 T. Vermonden, W. E. Hennink, H. Weinans, A. A. Zadpoor, and others,  
38 “Simultaneous Delivery of Multiple Antibacterial Agents from Additively  
39 Manufactured Porous Biomaterials to Fully Eradicate Planktonic and Adherent  
40 *Staphylococcus aureus*,” *ACS applied materials & interfaces*, vol. 9, no. 31, pp.  
41 25691–25699, 2017.
- 42 [13] G. Wang, W. Jin, A. M. Qasim, A. Gao, X. Peng, W. Li, H. Feng, and P. K. Chu,  
43 “Antibacterial effects of titanium embedded with silver nanoparticles based on  
44 electron-transfer-induced reactive oxygen species,” *Biomaterials*, vol. 124, pp. 25–  
45 34, 2017.

- 1 [14] M. N. Dickson, E. I. Liang, L. A. Rodriguez, N. Vollereaux, and A. F. Yee,  
2 “Nanopatterned polymer surfaces with bactericidal properties,” *Biointerphases*, vol.  
3 10, no. 2, p. 021010, 2015.
- 4 [15] T. Diu, N. Faruqui, T. Sjöström, B. Lamarre, H. F. Jenkinson, B. Su, and M. G.  
5 Ryadnov, “Cicada-inspired cell-instructive nanopatterned arrays,” *Scientific reports*,  
6 vol. 4, p. 7122, 2014.
- 7 [16] J. Hasan, S. Raj, L. Yadav, and K. Chatterjee, “Engineering a nanostructured ‘super  
8 surface’ with superhydrophobic and superkilling properties,” *RSC advances*, vol. 5,  
9 no. 56, pp. 44953–44959, 2015.
- 10 [17] F. D. Lowy, “Staphylococcus aureus infections,” *New England journal of medicine*,  
11 vol. 339, no. 8, pp. 520–532, 1998.
- 12 [18] R. G. Bailey, R. D. Turner, N. Mullin, N. Clarke, S. J. Foster, and J. K. Hobbs, “The  
13 interplay between cell wall mechanical properties and the cell cycle in  
14 Staphylococcus aureus,” *Biophysical journal*, vol. 107, no. 11, pp. 2538–2545, 2014.
- 15 [19] P. Eaton, J. C. Fernandes, E. Pereira, M. E. Pintado, and F. X. Malcata, “Atomic  
16 force microscopy study of the antibacterial effects of chitosans on Escherichia coli  
17 and Staphylococcus aureus,” *Ultramicroscopy*, vol. 108, no. 10, pp. 1128–1134,  
18 2008.
- 19 [20] S. Pogodin, J. Hasan, V. A. Baulin, H. K. Webb, V. K. Truong, V. Boshkovikj, C. J.  
20 Fluke, G. S. Watson, J. A. Watson, R. J. Crawford, and others, “Biophysical model of  
21 bacterial cell interactions with nanopatterned cicada wing surfaces,” *Biophysical  
22 journal*, vol. 104, no. 4, pp. 835–840, 2013.
- 23 [21] J. S. Milner, M. W. Grol, K. L. Beaucage, S. J. Dixon, and D. W. Holdsworth,  
24 “Finite-element modeling of viscoelastic cells during high-frequency cyclic strain,”  
25 *Journal of functional biomaterials*, vol. 3, no. 1, pp. 209–224, 2012.
- 26 [22] L. Wang, H.-Y. Hsu, X. Li, and C. J. Xian, “Effects of Frequency and Acceleration  
27 Amplitude on Osteoblast Mechanical Vibration Responses: A Finite Element Study,”  
28 *BioMed research international*, vol. 2016, 2016.
- 29 [23] C. Hartmann, K. Mathmann, and A. Delgado, “Mechanical stresses in cellular  
30 structures under high hydrostatic pressure,” *Innovative food science & emerging  
31 technologies*, vol. 7, no. 1–2, pp. 1–12, 2006.
- 32 [24] E. Zhou, C. Lim, and S. Quek, “Finite element simulation of the micropipette  
33 aspiration of a living cell undergoing large viscoelastic deformation,” *Mechanics of  
34 Advanced Materials and Structures*, vol. 12, no. 6, pp. 501–512, 2005.
- 35 [25] G. Francius, O. Domenech, M. P. Mingeot-Leclercq, and Y. F. Dufrêne, “Direct  
36 observation of Staphylococcus aureus cell wall digestion by lysostaphin,” *Journal of  
37 bacteriology*, vol. 190, no. 24, pp. 7904–7909, 2008.
- 38 [26] F. Xue, J. Liu, L. Guo, L. Zhang, and Q. Li, “Theoretical study on the bactericidal  
39 nature of nanopatterned surfaces,” *Journal of theoretical biology*, vol. 385, pp. 1–7,  
40 2015.
- 41 [27] Y. Jin, Y. Zhang, H. Ouyang, M. Peng, J. Zhai, and Z. Li, “Quantification of Cell  
42 Traction Force of Osteoblast Cells Using Si Nanopillar-Based Mechanical Sensor,”  
43 *Sensors and Materials*, vol. 27, no. 11, pp. 1071–1077, 2015.
- 44 [28] S. Janbaz, N. Noordzij, D. S. Widyaratih, C. W. Hagen, L. E. Fratila-Apachitei, and  
45 A. A. Zadpoor, “Origami lattices with free-form surface ornaments,” *Science  
46 advances*, vol. 3, no. 11, p. eaao1595, 2017.

- 1 [29] W. et al., “Towards osteogenic and bactericidal nanopatterns,” 2018.
- 2 [30] S. Wu, F. Zuber, J. Brugger, K. Maniura-Weber, and Q. Ren, “Antibacterial Au  
3 nanostructured surfaces,” *Nanoscale*, vol. 8, no. 5, pp. 2620–2625, 2016.
- 4 [31] J. J. Perry, J. T. Staley, S. Lory, and others, *Microbial life*. Sinauer Associates  
5 Incorporated, 2002.
- 6 [32] J. Thwaites and N. H. Mendelson, “Biomechanics of bacterial walls: studies of  
7 bacterial thread made from *Bacillus subtilis*,” *Proceedings of the National Academy  
8 of Sciences*, vol. 82, no. 7, pp. 2163–2167, 1985.
- 9 [33] F. Li, C. U. Chan, and C. D. Ohl, “Yield strength of human erythrocyte membranes to  
10 impulsive stretching,” *Biophysical journal*, vol. 105, no. 4, pp. 872–879, 2013.
- 11 [34] E. P. Ivanova, J. Hasan, H. K. Webb, G. Gervinskas, S. Juodkazis, V. K. Truong, A.  
12 H. Wu, R. N. Lamb, V. A. Baulin, G. S. Watson, and others, “Bactericidal activity of  
13 black silicon,” *Nature communications*, vol. 4, p. 2838, 2013.
- 14 [35] A. Tripathy, P. Sen, B. Su, and W. H. Briscoe, “Natural and bioinspired  
15 nanostructured bactericidal surfaces,” *Advances in colloid and interface science*, vol.  
16 248, pp. 85–104, 2017.
- 17 [36] S. Kim, U. T. Jung, S.-K. Kim, J.-H. Lee, H. S. Choi, C.-S. Kim, and M. Y. Jeong,  
18 “Nanostructured multifunctional surface with antireflective and antimicrobial  
19 characteristics,” *ACS applied materials & interfaces*, vol. 7, no. 1, pp. 326–331,  
20 2015.
- 21 [37] X. Li, “Bactericidal mechanism of nanopatterned surfaces,” *Physical Chemistry  
22 Chemical Physics*, vol. 18, no. 2, pp. 1311–1316, 2016.
- 23 [38] X. Li and T. Chen, “Enhancement and suppression effects of a nanopatterned surface  
24 on bacterial adhesion,” *Physical Review E*, vol. 93, no. 5, p. 052419, 2016.
- 25 [39] A. Mai-Prochnow, M. Clauson, J. Hong, and A. B. Murphy, “Gram positive and  
26 Gram negative bacteria differ in their sensitivity to cold plasma,” *Scientific reports*,  
27 vol. 6, p. 38610, 2016.
- 28 [40] M. T. Madigan and J. M. Martinko, “Microorganisms and microbiology,” *Brock  
29 biology of microorganisms. 11th ed. Upper Saddle River, New Jersey (NJ): Pearson  
30 Prentice Hall*, pp. 1–20, 2006.
- 31

1 **Figure captions**

2 **Figure 1.** a) A schematic drawing of *Staphylococcus aureus* and osteoblast and the  
3 dimensions used in our finite element models. b) The different parameters of nanopatterned  
4 structures including the height  $H$ , width,  $W$ , interspacing,  $IS$ , radius,  $r$ , and shape of the  
5 nanopillars. c) A schematic drawing displaying the positioning of the bacteria on  
6 nanopatterned structures.

7 **Figure 2.** The effects of different geometrical features including the (a) height,  $H$ , (b)  
8 interspacing,  $IS$ , (c) width,  $W$ , (d) shape, and (e) radius,  $r$  of the nanopillars on the sinking  
9 depth ratio,  $\frac{SD}{D}$ , and equivalent von Mises strain,  $\epsilon_{eq}$ .

10 **Figure 3.** a) The results of four numerical simulations of how osteoblasts interact with  
11 nanopillars. The geometrical features of each model are presented in Table S3. b) Normalized  
12 equivalent von Mises strain,  $\epsilon_{eq}$ , with respect to the rupture strain,  $\epsilon_{th}$ . c) A map of  
13 bactericidal and cytotoxic behaviors predicted for different dimensions of the nanopillars.  
14 The interspace and width are normalized to the diameter of bacteria. The Log-log plots of  
15 von Mises strain versus two normalized parameters (d)  $\frac{W}{W+IS}$  and (e)  $\frac{R}{IS}$ .

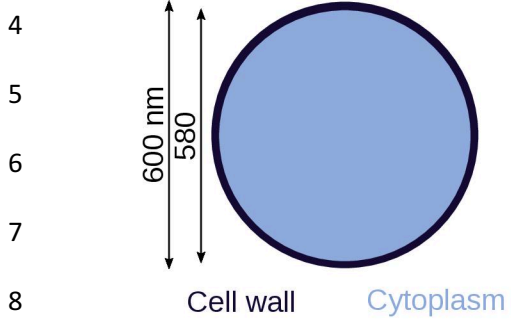
16

17

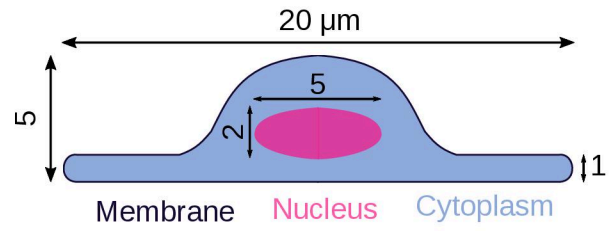
1 **Figure 1**

2

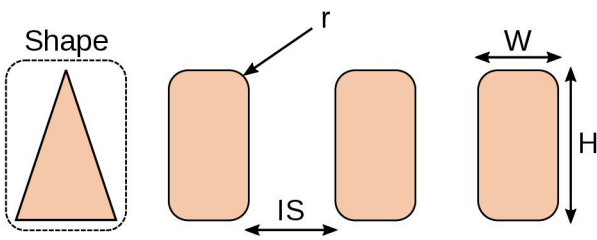
3 a) *Staphylococcus aureus*



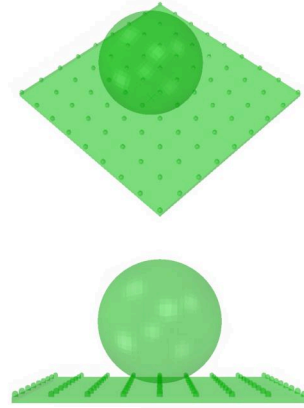
Osteoblast cell



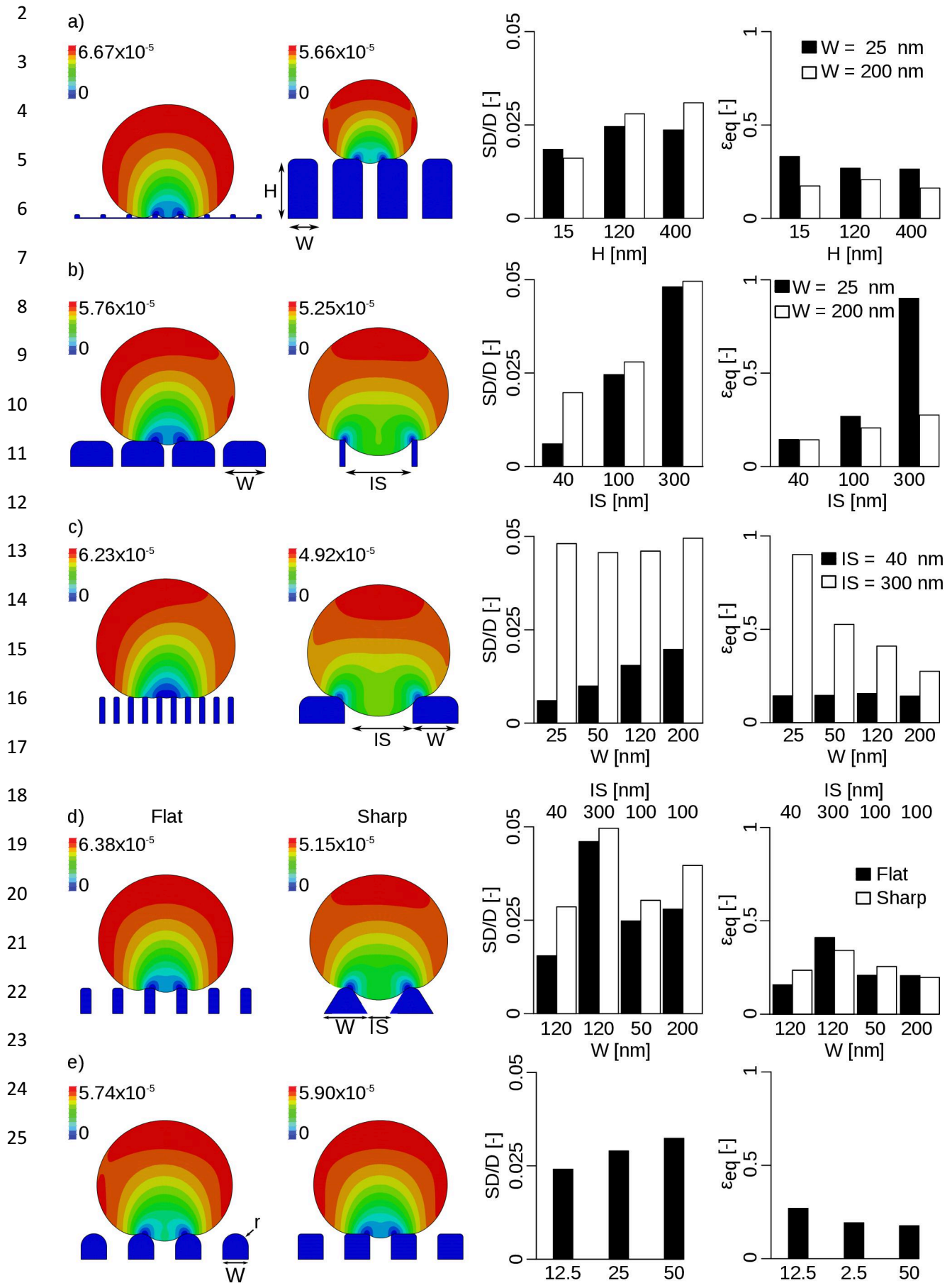
9 b)



c)



1 **Figure 2**



1 **Figure 3**

